INDO AMERICAN JOURNAL OF PHARMACEUTICAL RESEARCH

CHEMICAL SYNTHESIS OF METALLIC NANOPARTICLES AND ITS APPLICATION

N. Krithiga, A. Rajalakshmi, A. Jayachitra

Dept of Plant Bbiotechnology, School of Biotechnology, Madurai Kamaraj University Madurai 21.

ARTICLE INFO

Article history
Received 27/02/2017
Available online
14/03/2017

Keywords
Nanoparticles,
Antibacterial,
SEM,
TEM and *In Vitro*
Cytotoxicity.

ABSTRACT

In the developing world the metallic nanoparticles have been investigated because they exhibit unusual chemical properties, depending on their size and shape, larger surface area and thus opening many possibilities with respect to technological applications. The gold, silver and iron oxide nanoparticle are implicated for usagae of potential antioxidant and antimicrobial agents. Nanotechnology has elevated the standards of treatment for various disease especially for cancer. In the present work metallic nanoparticles were fabricated via the chemical synthesis route via chemical reduction and co precipitation technique. The synthesised nanoparticles were characterized using UV, FTIR, XRD, EDAX, SEM and TEM. The MIC and MBC values were determined further confirmed by resazurin assay and well diffusion method. The *in vitro* cytotoxicity were analyzed using Hep 2 and AGS cell line.

Corresponding author
N. Krithiga
Dept of Plant Bbiotechnology,
School of Biotechnology,
Madurai Kamaraj University Madurai 21.
gn.krithi@gmail.com

*Please cite this article in press as **N. Krithiga** et al. Chemical Synthesis of Metallic Nanoparticles and its Application. Indo American Journal of Pharmaceutical Research.2017:7(02).*

INTRODUCTION

One of the fields in which nanotechnology finds extensive applications is nanomedicine, an emerging new field which is an outcome of fusion of nanotechnology and medicine. Medicine is no more physician job exclusively, the materials and devices designed at the level of nanoscale are for diagnosis, treatment, preventing diseases and traumatic injury, relieving pain and also in the overall preservation and improvement of health[1].

Nanotechnology can improve our understanding of living cells and of molecular level interactions. A number of nanoparticles based therapeutics have been approved clinically for infections, vaccines and renal diseases**.** Oligodynamic silver having antimicrobial efficacy extends well beyond its virotoxicity and it have lethal effects spanned across all microbial domain[2]**.** The application of silver nanoparticles in drug delivery, drug discovery and new drug therapies have declare war on many dead full diseases and they use the body natural transport pathway and natural mechanism of uptake of the drug by the diseased cells[3].

Nanotechnology involves the production, manipulation and use of materials ranging in the size from less than a micron to that of individual atoms [4]. A wide variety of physical, chemical and biological methods are available for the synthesis of nanoparticles, some of these are very useful [5]**.**

Nanotechnology is the production and use of the smallest possible scale[6]. Nanoparticles have emerged as novel antimicrobial agents owing to the high surface area to volume ratio, which is coming up as the current interest in the researchers due to the growing microbial resistances against metal ions, antibiotics and the development of resistant strain [7]. Nanobiotechnology is the most active areas of research in modern material science. Nanoparticles exhibit completely new or improved properties based on specific characteristics such as size, distribution and morphology[8].

Bionanotechnology is the integration between biotechnology and nanotechnology for developing biosynthetic and ecofriendly technique for the synthesis of nanomaterials [9]. Recently, greater insights regarding the ecological impact of nanoparticles have become increasingly recognized as worthwhile goal. The toxic potential is due to their intrinsic toxic properties. Inorganic materials such as metal and metal oxides have attracted lots of attention over the past decade due to their ability to withstand harsh process condition[10].

MATERIALS AND METHODOLOGY

Chemicals required

Silver nitrate ($AgNO_3$),Auric chloride($HAuCl_4$), Iron(II) chloride tetrahydrate ($FeCl_2{\cdot}4H_2O$), iron(III) chloride hexahydrate ($FeCl_3{\cdot}6H_2O$), trisodium citrate, Glucose, sodium hydroxide (NaOH), ammonium hydroxide (NH_4OH), Glutaraldehyde, acetic acid, monobasic phosphate salt, Dibasic phosphate salt, deoxyribose, Sodium nitroprusside EDTA, nitroblue tetrazolium, riboflavin, thiobarbituric acid, sulphanilamide, phosphoric acid, napthylethylene diamine dihydrochloride, ascorbate, yeast extract, NaCl, peptone, Agar Agar,rezasurin dye, DPPH, Luria bertani broth, muller hinton agar, nutrient broth,DMEM,FBS, streptomycin (antibiotic solution), Trypsin EDTA solution, DMSO and MTT were purchased from Himedia .pvt.Ltd, India. All the reagents and buffers were prepared using deionised water.

The bacterial strains were procured from MTCC, Pune *Escherichia coli, Klebisella pneumoniae, Staphylococcus aureus* and *Streptococcus viridians* were used for the antibacterial studies .

Synthesis of gold nanoparticles

Gold nanoparticle was prepared using standard citrate reduction method [11]. 100 mL of 1 mM aqueous $HAuCl_4$ (Sigma, USA) solution was heated to 100 ºC under refluxing conditions. While stirring vigorously, 10 ml of 38.8 mM sodium citrate were added rapidly. The yellow solution became transparent and changed into wine red, indicates the formation of gold nanoparticle. The mixture was kept at 100 ºC for 15 minutes and subsequently cooled to room temperature with continuous stirring. The chemical mechanism of formation of gold nanoparticles after reduction and stabilization.

Synthesis of Silver nanoparticles

The silver nanoparticles were prepared by using chemical reduction method [12]. All solutions of reacting materials were prepared in double distilled water. In typical experiment 50ml of 1mM $AgNO_3$ was heated to boiling. To this solution 5ml of 1% trisodium citrate was added drop by drop. During this process solution was mixed vigorously and heated until colour change was evident (pale brown). Then it was removed from the heating element and stirred until cooled to room temperature. The aqueous solution air dried up to 3 days and produced the dry powdered particles that were taken for further analysis.

Synthesis of iron oxide nanoparticles

Co-precipitation is a facile and convenient way to synthesize iron oxides (either Fe_3O_4 or γ-Fe_2O_3) from aqueous (Fe^{3+}/Fe^{2+} 2:1 molar ratio) salt solutions by the addition of a base at room temperature or at an increased temperature. The magnetic nanoparticles were synthesized by the co precipitating method with minor modification[13]**.** $FeCl_3.6H_20$ (4.335mM) and $FeCl_2.4H_2O$(2.17mM) were dissolved in 50 ml of the double distilled water in a 250 ml three neck flask. Thereafter the reaction temperature was raised to 85°C and the above solution was stirred at 85°C for 30 min with N_2 as the protective gas, subsequently, $NH_3.H_2O$ (25ml) was added to the solution with vigorous stirring, and then sodium citrate (0.13mM) was immediately added when the color changed to black and the solution was stirred at 85°C for 30 mins. Finally, the magnetic Fe_3O_4 nanoparticles were obtained after magnetic separation and washed with distilled water to neutral pH.

Characterization of metallic nanoparticles:

UV-visible absorbance spectroscopy [14]

UV-Visible spectroscopy analysis was carried out on a Systronic UV-Visible absorption spectrophotometer 117 with a resolution of ±1nm between 200-1000nm processing a scanning speed of 200nm/sec. Maximum absorption of the UV-Visible spectra of metallic nanoparticles in aqueous solution with different wavelength in nanometers from 340 to 800nm.

X-ray diffraction (XRD) [15]

A thin film of the metallic nanoparticle was made by dipping a glass plate in a solution and carried out for X-ray diffraction studies. The crystalline silver nanoparticle was calculated from the width of the XRD peaks and the average size of the nanoparticles can be estimated using the Debye–Scherrer equation**.**

$$D = k\lambda / \beta\cos\theta$$

Where *D* = Thickness of the nanocrystal, *k* = Constant; λ = Wavelength of X-rays, ;β = Width at half maxima of (111) reflection at Bragg's angle 2θ,;θ = Bragg angle. The size of the silver nanoparticle was made from the line broadening of the (111) reflection using the Debye-Scherrer formula. Where, Constant (K) = 0.94; Wave length (λ) = 1.5406×10^{-10}

Scanning electron microscopy (SEM) and EDAX [16]

The pellet was subjected for SEM analysis. Thin films of the sample were prepared on a carbon coated copper grid by just dropping a very small amount of the sample on the grid, extra solution was removed using a blotting paper and then the film on the SEM grid were allowed to dry for analysis.

Free radical scavenging effect of metallic nanoparticles

DPPH photometric assay [17]

The ability of the synthesised metallic nanoparticles to bleach DPPH can be quantified using a spectrophotometric assay. The extent of scavenging causing a proportional change in the absorbance at 518nm.

Reagents required

- 0.4mM DPPH in Methanol
- Methanol

Procedure

1ml of the methanolic solution of DPPH was added with 1ml of metallic nanoparticles (usually a stock concentration of 1 mg/ml for metallic nanoparticles) at various concentrations of 10 - 50µg/ml and the tubes were allowed to stand at room temperature for 30minutes at dark condition. Methanol and DPPH mixture served as blank. After 30minutes, the absorbance was measured at 518nm and converted into percentage radical scavenging activity as follows.

% scavenging activity = (Blank – Sample) /blank X 100

Superoxide free radical generation [17]

The extent of superoxide generation was studied on the basis of inhibition of production of nitroblue tetrazolium formazone by the metallic nanoparticles solution was measured using spectrophotometer at 560nm.

Reagents required

- EDTA (0.1M containing 1.5 mg NaCN)
- Nitroblue tetrazolium (NBT, 1.5mM)
- Riboflavin (0.12mM)
- Phosphate buffer (0.06 M, pH 7.6)
- Dimethyl sulphoxide (DMSO)

Procedure

The metallic nanoparticles (usually a stock concentration of 1 mg/ml for metallic nanoparticles) was dissolved in 3ml of potassium phosphate buffer, centrifuged at 2000g for 10minutes and the supernatants were used for the assay. The assay mixture contained 1.2ml of sodium pyrophosphate buffer, 0.1ml of PMS, 0.3ml of NBT, 0.2ml of enzyme preparation and water in a total volume of 2.8ml. The reaction was initiated by the addition of 0.2ml NADH. The mixture was incubated at 30˚C for 90 seconds and arrested by the addition of 1ml of glacial acetic acid. The reaction mixture was then shaken with 4ml of n - butanol, allowed to stand for 10minutes and centrifuged. The intensity of the chromogen in the butanol layer was measured at 560nm in a spectrophotometer. One unit of enzyme activity is defined as the amount of enzyme that gave 50% inhibition of NBT reduction in one minute.

Hydroxyl radical scavenging [18]

The hydroxyl radical scavenging activity of the samples was quantified by the method reported by elizabeth and Rao (1990).

Reagents required

- Ferric chloride (0.1 mM)
- EDTA (0.1mM)
- H_2O_2 (1mM)
- Ascorbate (0.1mM)
- KH_2PO_4-KOH buffer (20mM, pH 7.4)
- Deoxyribose (2.8mM)
- Thiobarbituric acid (TBA, 1%)

Procedure

Hydroxyl radical scavenging (Elizabeth and Rao, 1990) The assay is based on quantification of the degradation product of 2-deoxyribose by condensation with TBA. Hydroxyl radical was generated by the Fe^{3+}-ascorbate-EDTA-H_2O_2 system (the Fenton reaction). The reaction mixture contained, in a final volume of 1 ml, 2-deoxy-2-ribose (2.8 mM); KH_2PO_4-KOH buffer (20 mM, pH 7.4); $FeCl_3$ (100 µM); EDTA (100 µM); H_2O_2 (1.0 mM); ascorbic acid (100 µM) and concentrations (500 µg/ml) of the test sample or reference compound. After incubation for 1 h at 37°C, 0.5 ml of the reaction mixture was added to 1 ml 2.8% TCA, then 1 ml 1% aqueous TBA was added and the mixture was incubated at 90°C for 15 min to develop the color. After cooling, the absorbance was measured at 532 nm against an appropriate blank solution. All tests were performed six times. Quercetin was used as a positive control. Percentage inhibition was evaluated by comparing the test and blank solutions.

$$\% \text{ scavenging of hydrogen peroxide} = (A_0 - A_1) \times 100 / A_0$$

D) Nitric oxide free generation in vitro [19]

Principle

Aqueous solution of sodium nitroprusside spontaneously generates nitric oxide (NO) at physiological pH, which interacts with oxygen to produce nitrite ions, which is measured spectrophotometrically at 546nm.

Reagents required

- Phosphate buffered saline (PBS), pH 7.2
- Sodium nitroprusside (100mM)
- Griess reagent (1% sulphanilamide, 2% phosphoric acid and 0.1% napthylethylene diamine dihydrochloride)

Procedure

The reaction mixture containing 0.3ml of sodium nitroprusside, 2.68ml PBS and 20µl of sample (usually a stock concentration of 1 mg/ml for metallic nanoparticles) was incubated at 25˚C for 15 minutes. Control tubes (100% generation) were prepared without the sample. After incubation, 0.5ml of the Griess reagent was added. The absorbance of the chromophore formed, indicative of the quantum of NO generated, was read at 546 nm.

Antibacterial activity of the chemically synthesized Au, Ag and Fe_3O_4 nanoparticles:

Nutrient broth (g/L)		Luria bertani broth (g/L)	
Peptone	--- 10.0g	Peptone	--- 5.0g
Sodium chloride	--- 5.0g	Beef extract	--- 3.0g
Yeast extract	---5.0g	Yeast extract	--- 3.0g
ddH_2O	--- 1000ml	Sodium chloride	---5.0g ddH_2O --- 1000ml

Minimum Inhibitory Concentration (MIC) [20]

Reagents required

Different concentrations (10 – 30 µg/ml) of metallic nanoparticles were prepared and mixed with 450 µl/ml of nutrient broth and 50 µl of 24 h old bacterial innoculum and allowed to grow overnight at 37°C for 48h. Nutrient broth alone served as negative control. Whole setup was performed in triplicate and was incubated at 37°C for 24 h.

Minimum Bactericidal Concentration (MBC) [20]

To avoid the possibility of misinterpretations due to the turbidity of insoluble compounds if any, the MBC was determined by sub culturing the above (MIC) serial dilutions after 24 h in nutrient agar plates using 10µl of culture was taken and plated followed by incubation at 37°C for 24 h.

Bacterial killing kinetics using nanosilver [21]

To examine the bacterial killing kinetics in the presence of metallic nanoparticles, a modified method described by [21] was followed. Since the following pathogens *Escherichia coli,, Pseudomonas aeruginosa, Staphylococcus aureus* and *Streptococcus viridans* and showed a better activity. The human bacterial pathogens were grown in 10ml of nutrient broth supplemented with different doses of nanoparticles (nanoparticle content 10, 20, 30, 40 and 50µg/ml) at 37°C without agitation. Killing kinetic rates and bacterial concentrations were determined by measuring the colony forming unit in the nutrient agar plates. Percentage of bacterial growth inhibition was calculated as per the equation of Shahi, *et al.,* 2003.

$$BGI\ \% = (BC - BT) \times 100 / BC$$

Where BGI = Bacterial Growth Inhibition; BC = Number of Bacterial Colonies

Resazurin dye reduction method [22]

Dye preparation

The resazurin solution was prepared by dissolving a 270 mg tablet in 40 ml of sterile distilled water. A vortex mixer was used to ensure that it was a well-dissolved and homogenous solution.

Procedure

Plates were prepared under aseptic conditions. A sterile 96 well plate was labeled. A volume of 100 µL of test material in 10% (v/v) sterile water (usually a stock concentration of 1 mg/ml for metallic nanoparticles) was pipette into the first row of the plate. To all other wells 50 µL of nutrient broth or normal saline was added. Serial dilutions were performed using a multichannel pipette. Tips were discarded after use such that each well had 50 µl of the test material in serially descending concentrations. To each well 10 µl of resazurin indicator solution was added. Finally, 10 µl of bacterial suspension (5×10^6 cfu/ml) was added to each well to achieve a concentration of 5×10^5cfu/ml. Each plate was wrapped loosely with parafilm to ensure that bacteria did not become dehydrated. Each plate had a set of controls; one column with a broad-spectrum antibiotic as positive control (usually ciprofloxacin in serial dilution), another column with all solutions with the exception of the test compound, and third column with all solutions with the exception of the bacterial solution then to all the three columns add 10 µL of nutrient broth and placed in an incubator at 37 °C for 18–24 h. The colour change was then assessed visually. Any colour changes from purple pink or colorless were recorded as positive.

Disc Diffusion Method [23]

Reagents required

Muller Hinton agar medium (g/1)

Beef extract	-300g
Casein acid hydrolysate	-17.5g
Starch	-1.5g
Agar	-17.0
Distilled water	-1000ml
pH	-7.3 ± 0.2

The Muller Hinton agar media was prepared and poured in the petriplates and kept for 30 minutes for solidification. After 30 minutes the fresh overnight cultures of various pathogens were taken and spread over the solidified Muller Hinton agar plates. Wells were made with sterile well puncture (filled with metallic nanoparticles from 20µg/ml **(**Au, Ag and Fe_3O_4 nanoparticles) along with standard antibiotic were placed in each plate. The cultured agar plate were incubated at 37^0C for 24 h. After 24 h of incubation the zone of inhibition was investigated.

***In vitro* studies *cy*totoxiocity studies**

The anti-cytotoxicity activity of the synthesized metallic nanoparticles was analyzed against Hep G2 and AGS cell line.

Culturing of cells

The Hep G2 and AGS cell line was obtained from NCCS, Pune. The cells were cultured in DMEM medium supplemented with FBS 10%, penicillin, 100 IU/ml, and streptomycin 100 mg/mL. The harvested cells were incubated in a Petri dish for one hour a 37°C in 5%, atmospheric CO_2, and adherent cells were cultured and used for *in vitro* experiments.

***In vitro* cell viability studies**

The MTT assay is a simple, nonradioactive colorimetric assay to measure cell viability. Metabolically active cells are able to convert this dye into a water-insoluble dark purple formazan by reductive cleavage of the tetrazolium ring. Formazan crystals, then, can be dissolved in an organic solvent such as dimethylsulphoxide (DMSO) and quantified by measuring the absorbance of the solution at 545 nm, and the resultant value is related to the number of living cells.

Reagents required

- MTT(5 mg/ml in phosphate buffer pH 7.4)
- DMSO

Procedure

For the determination of cell cytotoxicity /viability, the cells were plated at a density of (1x10 ^{6}cells/well) in a 96-well plate at 37˚C in 5% CO_2 incubator. After 24 h of culture, the medium in the wells was replaced with the fresh medium containing nanoparticles in varying concentrations. After 24 h, 20 µl of MTT dye solution (5 mg/ml in phosphate buffer pH 7.4) was added to each well. After 4 h of incubation at 37˚C and 5% CO_2, the medium was removed and formazan crystals were solubilized with 200 µl of DMSO and the solution was vigorously mixed to dissolve the reacted dye. The absorbance of each well was read on a micro plate reader at 545 nm. The spectrophotometer was calibrated to zero absorbance, using culture medium without cells. The relative cell viability (%) related to control wells containing cell culture medium without nanoparticles was calculated by the following formula:

% of cell viability = 100 x (Sample absorbance / Control absorbance)

Time of exposure assay

Cytotoxicity was also assessed using MTT assay at different time period. About 1×105 mL-1 cell lines in their exponential growth phase were seeded in a flat-bottomed 96-well plate. Gold nanoparticles with concentration 50 ȝg/mL were diluted in the growth medium and added to the plate. Incubations were carried out for various times (12, 24, 36, 48, 60 and 72 hr) at 37oC in an atmosphere of 5% CO2 in air. At the end of each incubation time 10µL of MTT reagent was added to each well and was further incubated for 4 hr. Formazan crystals formed after 4 hr in each well were dissolved in 150µL of detergent and the plates were read immediately in a micro plate reader (Bio-Rad micro plate reader-550) at 570nm. Untreated cell lines as well as the cell treated with gold nanoparticles at different time were subjected to the MTT assay for cell viability determination.

RESULTS AND DISCUSSION

The area of nanotechnology research is an emerging as a cutting edge technology interdisciplinary with biology, physics, chemistry, material science and medicine. Here we have followed the chemical synthesis where the size of the nanoparticles can be controlled by usage of reducing and stabilizing agents such that they can be implicated in various fields. The metallic nanoparticles Au, Ag and Fe_3O_4 nanoparticles were synthesized by chemical reduction method where the trisodium citrate act as reducing in the synthesis of AuNPs and AgNPs and for the synthesis of Fe_3O_4 NP co-precipitaion method was followed. The visual observation of colour change was noticed and taken for further characterization purpose.

Synthesis and characterization of Gold nanoparticles

The onset of nanoparticle synthesis in reaction mixture can be correlated with the variation in the color of the solution was observed. Appearance of bright red color indicates synthesis of monodispersed spherical AuNPs while appearance of purple or blue color indicates larger size of the NPs or agglomerated NPs.

Figure 1 (A) shows prominent colour change from yellow to red indicated the formation of gold nanoparticles and which was confirmed by the UV-Vis spectrum shown in Figure (1 (B)) where the surface Plasmon peak of gold nanoparticles was observed at 504nm.

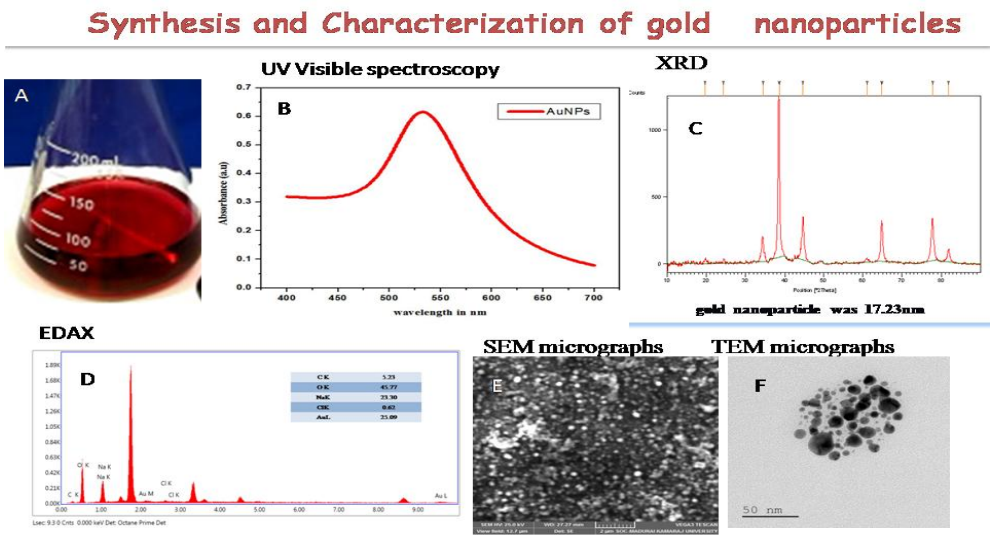

Figure 1 shows A) visual observation of colour change from yellow to red indicate the reduction of AU^{3+} to AU^{0}, B) UV visible spectrum, C) XRD spectrum, D) EDAX, E) SEM micrograph and F) TEM micrograph of gold nanoparticles.

Similarly earlier reports showed the mechanism of synthesis of monodispersed gold nanoparticles by the controlled reduction of an aqueous solution of tetrachloroauric acid. The Au^{3+} ions are reduced by the trisodium citrate to produce clusters of supersaturated Au^0 nuclei.

As the Au^0 concentration increases, they form seeds of nuclei and the particle growth occurs by further deposition of metallic gold upon the nuclei. The produced nanoparticle has a negative charge on its surface. Here the citrate anion acts both as a reducing as well as a capping agent. UV visible absorption spectra of synthesized AuNPs showed the characteristic absorption peak of AuNPs at 504 nm absorption peak or in other words the peak broadening represents the polydispersity of the synthesized nanoparticles or mixture of nanostructures. Size controlled preparation of gold nanoparticles was reported by [24] from 16nm to 147nm by varying the ratio between the reducing and stabilizing agents.

In Figure 1 (C) shows the XRD spectrum of the silver nanoparticles was analysed from te obtained 2θ values in the debye scheer's formula the average size of the nanoparticles was calculated and found to be 17.23nm, very small particles can also be produced

With this method by the use of strong reductants depending on the synthetic conditions adopted [25]. Figure1 (D) shows the EDAX profile where the presence of gold (25.07%) was confirmed Figure 1 (E) shows the SEM micrograph was observed and the shape was found to be spherical in nature and cluster of the nanoparticles was observed and Figure 1 (F) shows the TEM micrograph showed clustered spherical nanoparticles which was in accordance with that of the SEM micrograph. In most of the methods the sodium citrate reduction method produces a uniform size distribution of nanoparticles [26] .Spherical nanoparticles of gold showed an average diameter of 24 nm, respectively. However, the usage of nanomaterials in any application or any industry is highly dependent on synthesis of monodispersed particles of a particular morphology.

Synthesis and characterization of silver nanoparticles

Silver nanoparticles were synthesized according to the method described by [11] where the colloidal solution colourless solution turned pale brown, and then to black indicating that the silver nanoparticles were formed.

The visual observation of colour change was noticed in Figure 2 (A) and taken for the characterization Figure 2 (B) UV-Vis spectroscopy shows the surface Plasmon peak of silver nanoparticles 420 nm , The controlled synthesis mechanism proposed on the basis of AgNPs synthesis was validated through silver nanoparticles (AgNPs) synthesis. AgNPs synthesis was taken as model system for validating the hypothesis, since it is a major challenge to synthesize stable monodispersed silver nanostructures via chemical synthesis route. Silver nitrate ($AgNO_3$) was used as precursor, whereas trisodium citrate not only behaved as reducing agent but also helps in stabilizing the high surface energy particles from agglomeration. Synthesis was performed by taking precursor and reducing agent concentrations as reported in literature. The color of the reaction mixture changed from colorless to yellow and finally to black depicting the presence of uniform facet nanostructures. The absorption spectrum between 400-450 nm is usually the characteristic of the silver nanoparticles.

Further, [26] reported that Silver nanoparticles exhibited Yellowish brown colour in aqueous solution due to excitation of surface plasmon vibrations in silver nanoparticles.

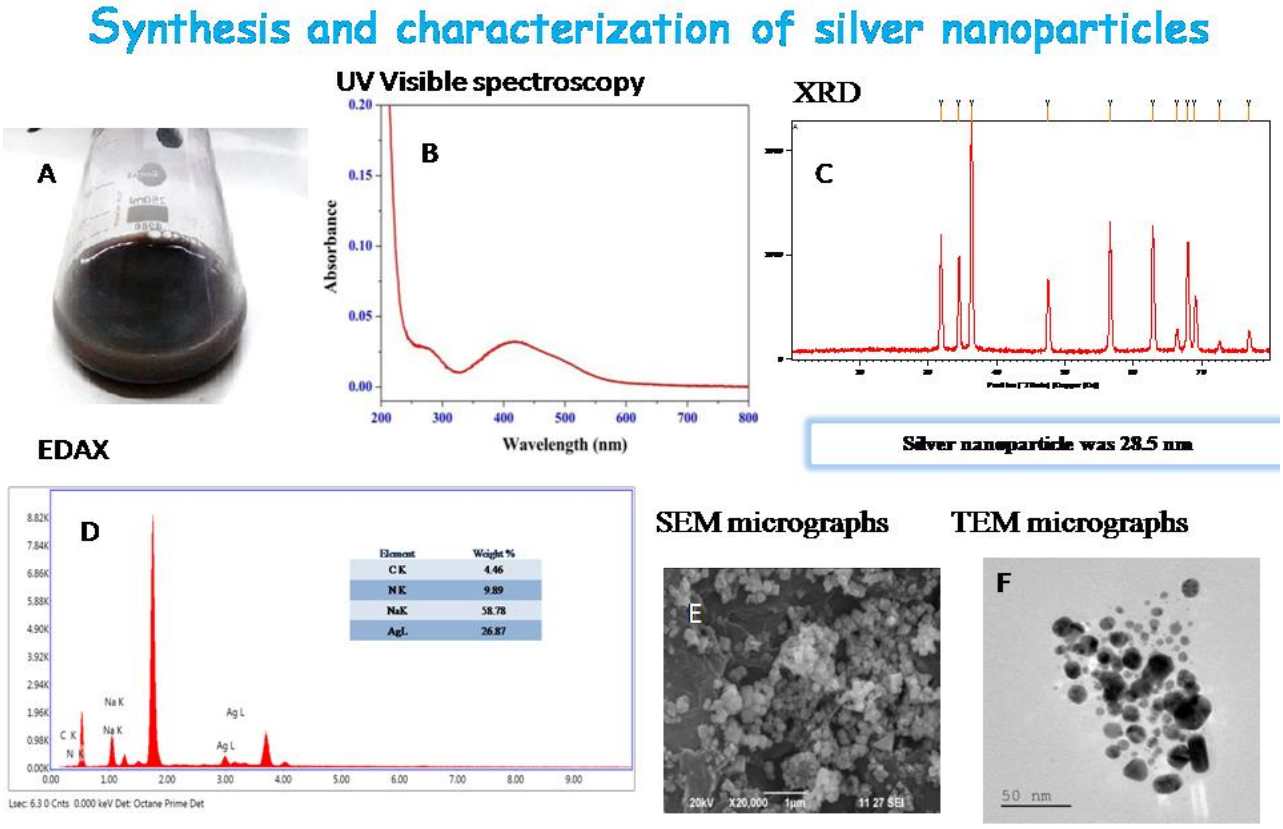

Figure 2 shows A) visual observation of colour change from yellow to red indicate the reduction of Ag^{+} to Ag^{0} ,B) UV visible spectrum, C) XRD spectrum, D) EDAX, E) SEM micrograph and F) TEM micrograph of silver nanoparticles.

In Figure 2 (C) shows the XRD spectrum was analysed from that using debye scheer's formula the calculated average size was found to be 28.5nm, In Figure 2 (D) shows the EDAX profile which confirms the presences of silver (26.87%), Figure 2 (E) SEM micrograph was observed and the shape was found to be round in nature The scanning electron micrograph of silver nanoparticles is depicted and the micrograph shows that the particles have a spherical nature and size ranges from 21.22+ 5.17,[14] and this is in accordance to results observed. SEM image of synthesised silver NPs by glucose which are spherical in shape and have a smooth surface morphology. It is also apparent that resulting NPs are more and less uniform in size and shape.

Figure 2(F) TEM micrograph also observe similar result of clustered round nanoparticles. The results by TEM indicate that the nanoparticles consist of agglomerates of small grains with mean diameters between 25 and 29 nm. However, some particles whose diameters are longer than 30 nm were formed because of aggregation during preparation is clearly seen in SEM micrographs. Where as in the TEM micrograph shows lesser agglomerates of small grains and some dispersed nanoparticles which are more or less spherical.

Synthesis and characterization of iron oxide nanoparticles

In figure 3 A shows the visual observation of colour change was noticed and taken for the characterization here we can see that the concentration of equilibrium with the solution as a function of temperature for various pH conditions, which are equivalent to various amounts of NaOH added during co-precipitation. And then a ratio of Fe^{3+} to Fe^{2+} equal to 2:1 is considered as the best condition achieved at room temperatures, which give the largest window of pH values, from 10.0 to 13.0, where a near perfect 2:1 stoichiometric solid may be produced. The dominant solids of Fe^{3+} and Fe^{2+} ions start to deviate from 0.1 and 0.05M at pH values greater than 12.0 or 13.0, depending upon temperature. pH values less than 12.0, and this ratio starts to deviate from 2.0 at pH values greater than 12.0. This is contrary to the method of increasing pH (OH^{-} concentration) to high values in order to completely precipitate the iron species as hydroxides that is used by experimentalists. These results justify the reason for which all the syntheses have been performed at room temperature.

Figure 3 (B) UV-Vis spectroscopy shows the surface Plasmon peak of iron nanoparticles 380 nm, Figure 3 (C) shows the XRD spectrum was analysed from that using debye scheer's formula the calculated average size was found to be 26.9 nm. In Figure 3 (D) EDAX profile shows and confirms the presences of iron (15.79%) Figure 3 (E) SEM micrograph was observed and the shape was found to be spherical in nature and Figure 3(F) TEM micrograph also observe similar result of polygonal nanoparticles.

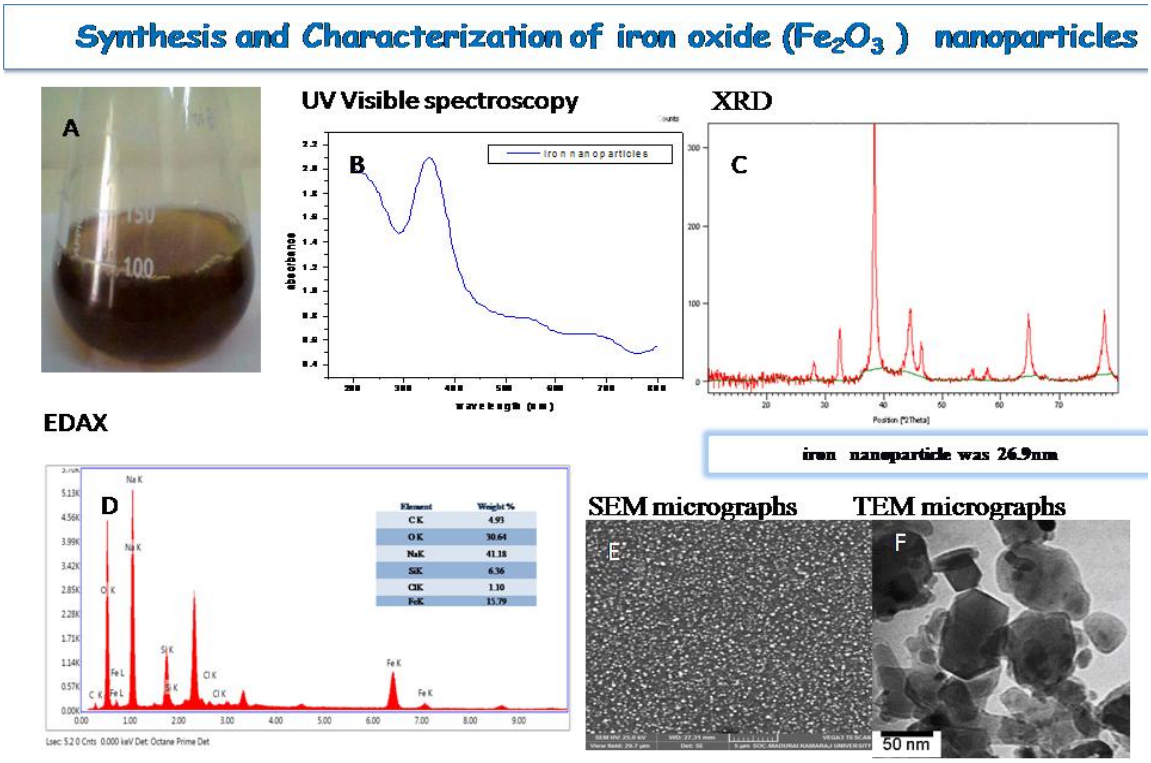

Figure 3 shows A) visual observation of colour change from green to dark brown or black indicate the Co precipitation method of Fe^{2+} and Fe^{3+} ,B) UV visible spectrum, C) XRD spectrum, D) EDAX, E) SEM micrograph and F) TEM micrograph of Iron(Fe_3O_4) nanoparticles.

Antioxidant property of metallic nanoparticles

A free radical has one or more unpaired electrons. An electron without a partner is highly unstable and very reactive. To gain stability, a free radical attacks another stable but vulnerable compound and steals an electron. After losing an electron, the previously stable molecule becomes a free radical and then it attacks another molecule stealing an electron. This process results in an electron-stealing chain reaction with one free radical producing another free radical.

The main characteristic of an antioxidant is its ability to trap free radicals. Many reactive oxygen species (ROS) including the hydroxyl radical, hydrogen peroxide and the peroxide radical are known to cause oxidative damage to living systems. ROS also play a significant role in human diseases such as cancer, atherosclerosis, hypertension and arthritis [27].

Free radicals especially damage polyunsaturated fatty acids in lipoproteins and in cell membranes, affecting transport of compounds in and out of cells. Free radicals also damage cell proteins (altering functions) and DNA (creating mutations). If free radical damage, oxidative stress, becomes extensive, health problems can develop. Oxidative stress has been identified as a causative factor in cognitive performance, the aging process, and in the development of diseases such as cancer, arthritis, cataracts, and heart disease (Richard, *et al.*, 1988).

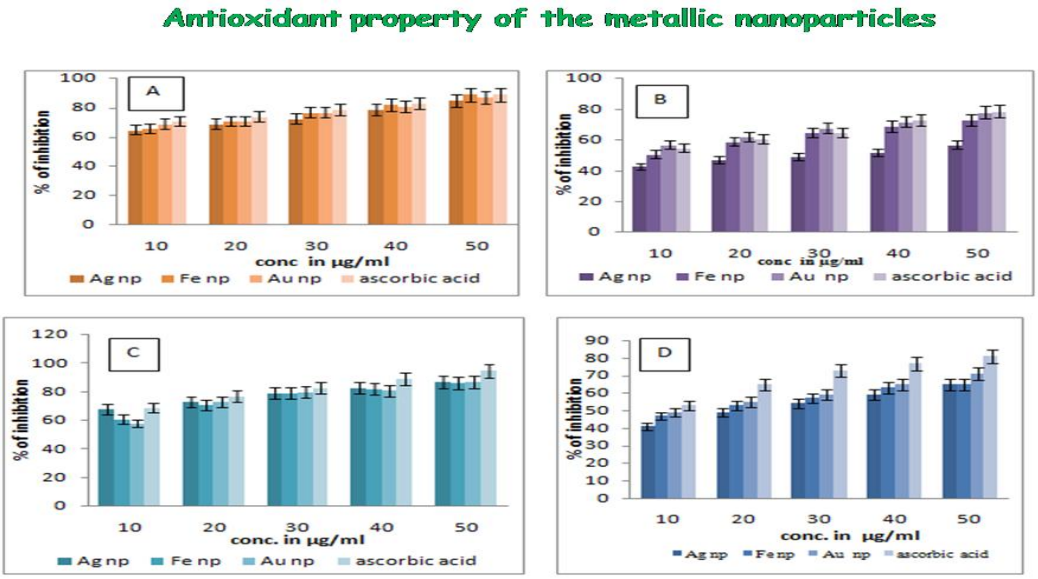

Figure 4 A) DPPH activity, B) Superoxide radical scavenging activity, C) Hydroxyl radical scavenging activity and D) Nitric oxide radical scavenging activity.

Figure 4 A, B, C and D shows the antioxidant and free radical scavenging effect where the concentration of the nanoparticle increases with increase in % of inhibition. This shows that the metallic nanoparticles have potential activity.

Free reducing sugars and reducing monosaccharides were not detected in the aqueous extract of Indian green tea implying that this plant is good for consumption for people suffering
from diabetes. The presence of phenolic compounds in this plant contributed to their antioxidative properties. The antioxidant activities of the plant were confirmed by performing various antioxidant assays. Nanoparticles and their ions (Iron and silver) can produce free radicals, resulting in induction of oxidative stress (i.e., Reactive Oxygen Species (ROS)) [28]. The main mechanism by which antibacterial drugs and antibiotics work is via oxidative stress generated by Reactive Oxygen Species which include superoxide radicals(O_2^-),
hydroxyl radicals (- OH), hydrogen peroxide (H_2O_2), and singlet oxygen (1 O2), causing damage to proteins, membrane, mitochondria and DNA in bacteria [29] and resulting in bacterial death. Fe^{2+} reacts with oxygen to create hydrogen peroxide, this H_2O_2 consequently reacts with ferrous iron via the Fenton reaction and produces hydroxyl radicals which are known to amage biological macromolecules.

Hence there is a potential candidate for multiple adverse interactions such as oxidative stress and inflammatory responses. Such cellular processes may lead to cell death via cell necrosis or apoptosis. The present study is useful towards authenticating the metallic nanoparticles to be potent antibacterial agents with several advantages such as low cost, easy preparation, and high reactivity compared to other metal nanoparticles.

Antibacterial activity of metallic nanoparticles

The mechanisms of NPs inhibiting bacterial growth remain unclear. It has been reported that the size and shape of NPs could affect their antibacterial activity[30].Studies suggested four mechanisms are hypothesized forantibacterial activity and these are firstly, accumulation and dissolution of nanoparticles in the bacterial membrane changing its permeability, with subsequent release of different intracellular biomolecules and dissipation of the proton motive force across the plasma membrane [31]. Second is generation of reactive oxygen species (ROSs) in the cell by NPs, with subsequent oxidative damage to cellular structures[32]. Third is uptake of nanoparticles and/ or metallic ions into cells, followed by depletion of intracellular ATP production, disruption of DNA replication and DNA damage and fourth is nanoparticles and its active ions which bind with different enzymes and inactivate them, resulting in arrest of cellular respiration [33-36] The nanoparticles get attached to the cell membrane and also penetrate inside the bacteria and form reactive oxygen species (ROS). So, recent studies suggested that generating reactive oxygen species, damaging cellular enzymes (cellular respiratory chain), disrupting cellular membrane, and DNAdamage ultimately lead to cell lysis and death.

The antibacterial activity of the metallic nanoparticles were analysed by a)MIC and C, resazurin dye reduction and disc diffusioin method. The MIC and MBC values are tabulated in **Table .1** shows the Minimum inhibitory concentration(MIC) and Minimum Bactericidal concentration (MBC) values of AuNP against pathogens were observed (i.e. in the range of 14-18µg/ml). The MIC and MBC of AuNP, AgNP and Fe_3O_4 NP shows potential activity at concentration ranging from 30-40 µg/ml.

The interrupted results from the **Table 1** clearly shows the effect of chemically synthesised metallic nanoparticles against the selected four pathogens .From the obtained data for the MIC and MBC against the various pathogens were analyzed for the AuNPs (gold nanoparticles) it was proved that the gram negative and gram positive microorganisms was found to be in the range of 10- 15 µg/ml of AuNPs. When the MBC datas where analyzed it showed good effect in the concentration of 30-40 µg/ml of AuNPs

Table 3.1 MIC & MBC of the AuNP, AgNP and Fe_3O_4 NP.

Name of the pathogens	*Klebisella pneumoniae*		*Staphylococcus auerus*		*Escherichia coli*		*Streptococcus viridians*	
Metallic nanoparticles	**MIC (µg/ml)**	**MBC (µg/ml)**	**MIC (µg/ml)**	**MBC (µg/ml)**	**MIC (µg/ml)**	**MBC (µg/ml)**	**MIC (µg/ml)**	**MBC (µg/ml)**
Au NPs	15	30	18	40	10	50	15	40
Ag NPs	16	30	11	35	13	40	16	35
Fe NPs	18	32	13	45	12	50	13	50

Table 3.1 shows the MIC & MBC of the AuNP, AgNP and Fe_3O_4 NP against the *Pseudomonas aeruginosa, Staphylococcus aureus, Escherchia coli and Streptococcus viridians*

From the obtained data for the MIC and MBC against the various pathogens were analyzed for the AgNPs (silver nanoparticles) it was proved that the gram negative and gram positive microorganisms was found to be in the range of 11- 16 µg/ml of AgNPs. When the MBC datas where analyzed it showed good effect in the concentration of 30-40 µg/ml of AgNPs, from the observation it was proved that the silver nanoparticles were more potentially active than the gold nanopartilces, So the silver nanoparticles can be used as a effective antibacterial agent.

From the obtained data for the MIC and MBC against the various pathogens were analyzed for the Fe_3O_4 NPs (Iron oxide nanoparticles) it was proved that the gram negative and gram positive microorganisms was found to be in the range of 12-18 µg/ml of Fe_3O_4 NPs . When the MBC values were analyzed it showed good effect in the concentration of 32- 50µg/ml of Fe_3O_4 NPs. Though the Fe_3O_4 NPs can act as antibacterial agent at a lower concentration as the concentration increases it does not produce more effect when compared with gold and silver nanoparticles.

Table 2 A shows the Bacterial Killing Kinetics was determined by calculating the colony forming unit in the culture. It was observed that the AuNP exhibit the killing rate of *Klebisella pneumoniae to* 77.6%, *Staphylococcus aureus* to 82.6%, *Escherichia coli* to 74.1% and *Streptococcus viridans* to 67.2% of viability for the AuNP. The correlation coefficient between AuNP and selected bacterial pathogens is provided in Table 2 B. It revealed that there is a strong positive correlation of AuNP against selected pathogens

Such as *Klebisella pneumonia, Staphylococcus aureus, E.coli* and *Streptococcus viridans* (0.9557, 0.9669, 0.9475 and 0.9981 respectively).

In table 3A AgNP exhibited the killing rate of *Klebisella pneumonia to* 81.7%, *Staphylococcus aureus* to 71.2%, *Escherichia coli* to 68.9% and *Steptococcus viridans* to 65.6% The correlation coefficient between AgNP and selected bacterial pathogens is provided in Table 3 B. It revealed that there is a strong positive correlation of AgNP against selected pathogens such as *Klebisella pneumonia, Staphylococcus aureus, E.coli* and *Streptococcus viridans* (0.9791, 0.9994, 0.9899, 0.9970).

Fe_3O_4 NP exhibited the killing rate of *Klebisella pneumoniae to 81.7%, Staphylococcus aureus* to 71.2%, *Escherichia coli* to 68.91% and *Streptococcus viridans* to 65.6% of viability for the Fe_3O_4 NP shown in Table 4 A. The correlation coefficient between and selected bacterial pathogens is provided in Table 4 B. It revealed that there is a strong positive correlation of Fe_3O_4 NP against selected pathogens such as *Klebisella pneumonia, Staphylococcus aureus, E.coli* and *Streptococcus viridans* (0.9729,0.9809,0.9497 and 0.9903 respectively), which interfers that as the concentration of the nanoparticles increase the bactericidal activity also increase.

Table 2(A) Bacterial killing kinetics for AuNP.

AuNP (µg/ml)	*Klebisella pneumoniae*	*Staphylococcus auerus*	*Escherichia coli*	*Streptococcus viridans*
0	260	276	240	290
5	205 (21.1%)	200(27.5%)	180(25%)	220 (24.1%)
10	169 (35%)	174(36.9%)	164(31.6%)	196 (32.4%)
15	136 (47.6%)	150(45.6%)	148(38.3%)	157 (45.8%)
20	108 (58.4%)	120(56.5%)	124(48.3%)	128 (55.8%)
25	58 (77.6%)	48(82.6%)	62(74.1%)	95 (67.2%)

Table 2(B) Correlation coefficient of AuNP against pathogens.

Correlation	'r' value
AuNP Vs *Klebisella pneumonia*	0.9957
AuNP Vs *Staphylococcus auerus*	0.9669
AuNP Vs *Escherichia coli*	0.9475
AuNP Vs *Streptococcus viridians*	0.9981

Table 3(A): Bacterial killing kinetics for AgNPs.

AgNPS (µg/ml)	*Klebisella Pneumonia*	*Staphylococcus auerus*	*Escherichia Coli*	*Streptococcus viridians*
0	274	264	280	285
5	246(10.2%)	225(14.7%)	240(14.2%)	250(12.2%)
10	213(22.2%)	186(29.5%)	190(32.1%)	202(29.1%)
15	173(36.8%)	151(42.8%)	176(37.1%)	168(41.0%)
20	135(50.7%)	117(55.6%)	125(55.3%)	136(52.2%)
25	85(81.7%)	76(71.2%)	87(68.9%)	98(65.6%)

Table 3 (B): Correlation coefficient of AgNPs of against pathogens.

Correlation	'r' value
AgNPs Vs Klebisella pneumonia	0.9791
AgNPs Vs *Staphylococcus auerus*	0.9994
AgNPs Vs *Escherichia coli*	0.9899
AgNPs Vs *Streptococcus viridians*	0.9970

Table 4 (A) : Bacterial killing kinetics for Fe_3O_4 NP.

Fe_3O_4 NP (µg/ml)	*Klebisella pneumoniae*	*Staphylococcus Auerus*	*Escherichia Coli*	*Streptococcus viridians*
0	274	264	280	285
5	205 (21.1%)	200(27.5%)	180(25%)	220 (24.1%)
10	213(22.2%)	186(29.5%)	190(32.1%)	202(29.1%)
15	136 (47.6%)	150(45.6%)	148(38.3%)	157 (45.8%)
20	108 (58.4%)	120(56.5%)	124(48.3%)	128 (55.8%)
25	85(81.7%)	76(71.2%)	87(68.9%)	98(65.6%)

Table 4 (B) Correlation coefficient of Fe_3O_4 NP of against pathogens.

Correlation	'r' value
Fe_3O_4 NP Vs *Klebisella pneumonia*	0.9729
Fe_3O_4 NP Vs *Staphylococcus auerus*	0.9809
Fe_3O_4 NP Vs *Escherichia coli*	0.9497
Fe_3O_4 NP Vs *Streptococcus viridans*	0.9903

The antibacterial studies of the chemogenic metallic nanoparticles was studied against two gram positive and gram negative using the resazurin dye method where the resazurin is an oxidation- reduction indicator which evaluates the cell growth. The change in colour from dark blue to pink indicate no inhibition, dark blue remaining indicate inhibition of cell growth. In this method the observed results where the dark blue indicate the level of inhibition for various metal oxide nanoparticles against various microorganism (Figure 5 A,B & C).

In Figure 6 The synthesized metallic nanoparticles posses potential antibacterial activity. The zone of inhibition (mm) were observed. The different concentration (20 µg/disc) of the prepared metallic nanoparticle zone of inhibition in the Y-axis and the various pathogens was taken in the X-axis. Thus, the graph was plotted.

The observed results were in accordance to the Earlier reports evaluated the functional AuNP antimicrobial activities on a laboratory strain (*Escherichia coli* DH5α), using broth dilution methods to determine the minimal inhibitory concentrations (MICs). AuNPs were incubated with 5 $X10^5$ cfu/mL of *E.coli* overnight. All AuNPs were able to completely inhibit the proliferation of *E. coli* at nanomolar concentrations; the MICs of different AuNPs, however, varied by the R group. To correlate antimicrobial activity with AuNP surface functionality, we plotted the MICs against the calculated AuNP end group log P values that quantitatively represent the relative NP surface hydrophobicity [35-36].

The present study clearly indicates that the prepared silver nanoparticles show good antibacterial activity against both gram negative and positive organism. As much the concentration of Ag nano particle increases there is significant increase in the antibacterial activity. In this study, the lowest concentration of Ag nanoparticles 20 µg/mL shows measureable cell growth on agar plates. Some researchers have reported that the antimicrobial effect of silver nanoparticles on Gram-negative bacteria was dependent on the concentration of Ag in the nanoparticles and was closely related to the formation of "pits" in the cell walls.

Antibacterial activity by resazurin dye reduction method.

Figure 5 A) Antibacterial activity of gold nanoparticles.

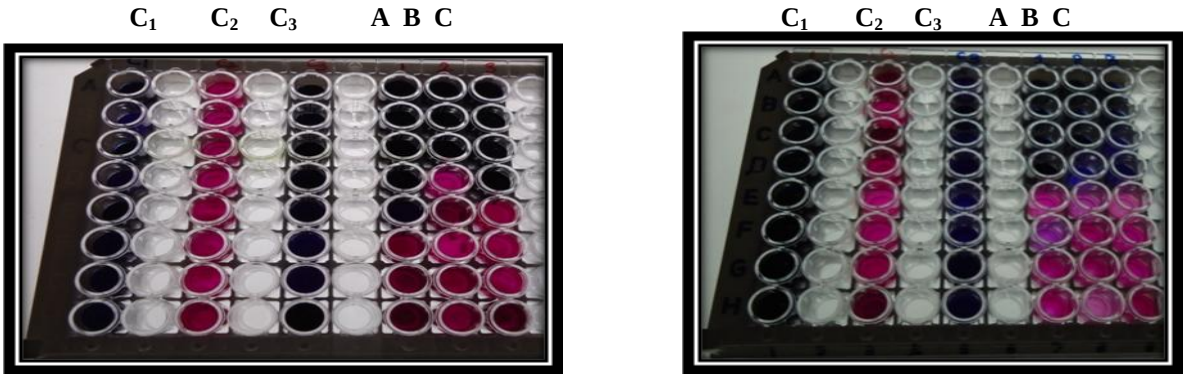

E.coli ***Staphylococcus aureus***

C_1 - Dye control **C_2** – ve control and **C_{3+}** ve control and **A**, **B** and **C** are the test samples at serial dilution

Figure 5 B) Antibacterial activity of silver nanoparticles.

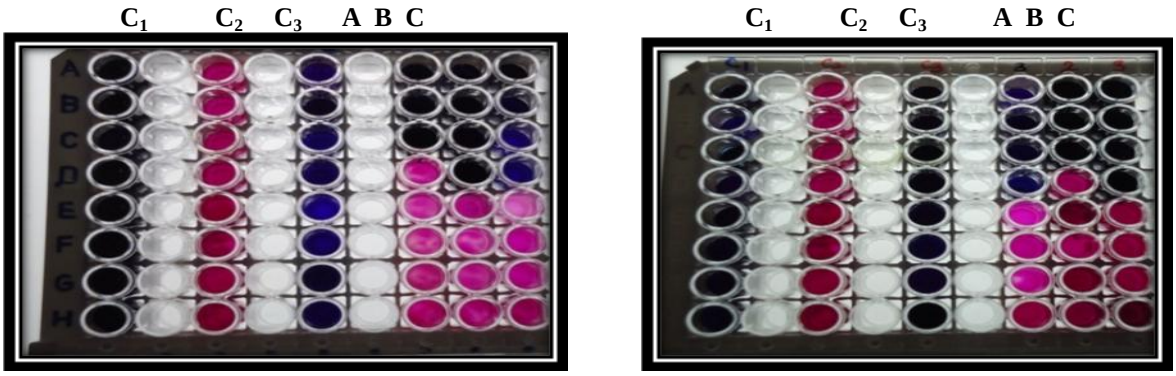

E.coli ***Staphylococcus aureus***

C_1 - Dye control **C_2** – ve control and **C_{3+}** ve control and **A**, **B** and **C are** the test samples at serial dilution

Figure 5 C) Antibacterial activity of iron oxide (Fe_2O_3)nanoparticles

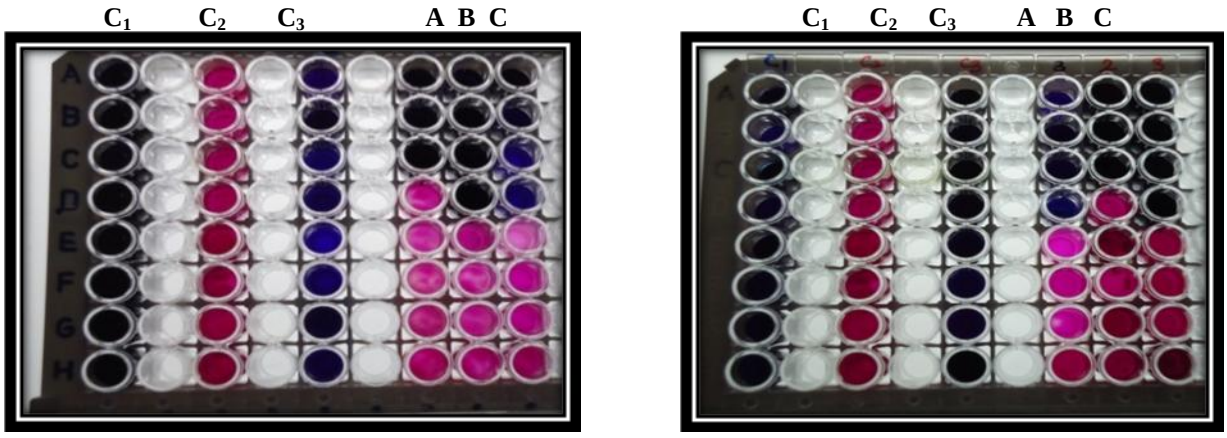

E.coli ***Staphylococcus aureus***

C_1 - Dye control **C_2** – ve control and **C_{3+}** ve control and **A**, **B** and **C** are the test samples at serial dilution

Figure 5 shows the colour changes observed for the antibacterial activity with resazurin dye reduction method A) AuNPs B) AgNPs and C) Fe_2O_3 NPs

Antibacterial activity of the metallic nanoparticle in well diffusion method.

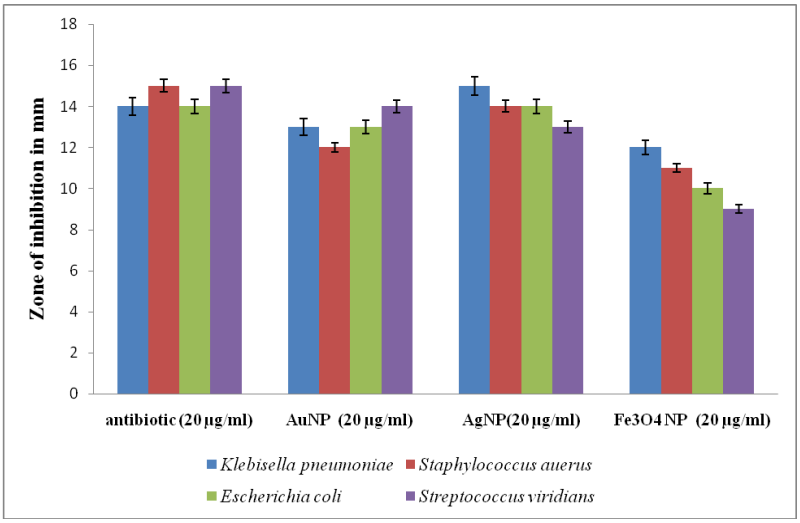

Figure 6 shows the zone of inhibition observed for various pathogens where the positive control ciprofloxacin and negative control 0.25% of DMSO.

The major mechanism through which silver nanoparticles manifest antibacterial properties was either by anchoring or penetrating the bacterial cell wall, and modulating cellular signaling[37]**.**However, the general mechanism of antibacterial activity of silver nanoparticles was proposed by many researchers, but the detailed mechanism remains to be understood.

Recently, it was reported that the antibacterial activity of Ag nanoparticles is related to the formation of free radicals [38]. Under certain conditions, high levels of Reactive Oxygen Species (ROS) can increase the oxidative stress in cells. Oxidative stress can not only cause damage to the cell membrane, but also cause damage to the proteins, DNA, and intracellular systems such as the respiratory system.

The bacterial growth was inhibited by silver ions, which accumulated into the vacuole and cell walls as granules. Silver nanoparticles may attach to the surface of the cell membrane and disturb its power function such as permeability and respiration functions followed by dysfunction of metabolic pathways; silver ions can interact with nucleic acids they preferentially interact [39]**.**It is reasonable to state that the binding of the particles to the bacteria depends on the surface area available for interaction. Smaller particles having the larger surface area available for interaction will give more bactericidal effect than the larger particles.

The antibacterial activity is probably derived, through the electrostatic attraction between negative charged cell membrane of microorganism and positive charged nanoparticles. Further the variation in the sensitivity between the gram positive and gram negative against the nanoparticles varies greatly. This might be due to the membrane permeability [40]**.**

The inhibitory effect of silver on microorganisms tested is effected via two possible mechanisms First, is the electrostatic attraction between the negatively charged cell membrane of the microorganisms and the positively charged Ag, and second, is the formation of pits in the cell wall of bacteria related to Ag concentration [41]**.**

The differences observed in the diameter of the zone of inhibition may be due to the difference in the susceptibility of different bacteria to the prepared silver nanoparticles. The differential sensitivity of gram negative and gram positive bacteria towards silver nanoparticles possibly depends upon their cell structure, physiology, metabolism and their interaction with the charged silver nanoparticles [42].

Effective antibacterial agents should be toxic to different pathogenic bacteria with the ability to be coated as antimicrobial coating on variety of surfaces like wound dressings, medical appliances, biomaterials, purifying and purity testing devices, textiles, biomedical and food packaging, consumer products and so on.

As much as the concentration of Fe nanoparticles increases, there is no such significant increase in the antibacterial activity. In this study, even the lowest concentration of Fe nano particle shows measureable inhibition effect. The presence of an inhibition zone clearly indicates the mechanism of the biocidal action of nanoparticles involved disrupting the membrane. Extending of inhibition depends on the concentration of nanoparticles as well as on the initial bacterial concentration. The reason could be that the smaller size of the particles which leads to increased membrane permeability and cell destruction [43].

The inactivation of bacteria by iron nanoparticles could be because of the penetration of the small particles into membranes of the bacteria. It is reasonable to state that binding of the nanoparticles to the bacteria depend on the surface available for interaction. Smaller particles having large surface area available for interaction will give more bactericidal effect than the larger particles [44].Because of the large surface area of the nanoparticles, it could be tightly adsorbed on the surface of the bacterial cells so as to disrupt the membrane, which would lead to the leakage of intracellular components, thus killing the bacterial cells[45]**.**

Iron nanoparticles could then react with intracellular oxygen, leading to oxidative stress and eventually causing disruption of the cell membrane and disturb its power function such as permeability and respiration functions followed by dysfunction of metabolic pathways including, and they can preferentially interact with nucleic acids. One possible explanation of the antibacterial effect is that the ions released by the nanoparticles may attach to the negatively charged bacterial cell wall and rupture it, thereby leading to protein denaturation and cell death [46]

The nanoparticles may also penetrate the cell and affect cellular respiration through inactivating the essential enzymes by forming complications with the catalytic sulfur of thiol groups in cysteine residues and through the production of toxic radicals such as superoxide, hydrogen peroxide, and hydroxyl ions.

Cell viability was calculated as the percentage of the viable cells compared to the untreated controls. The result shows that after 12 hour exposure to metallic nanoparticles, the viability started to decline.

In our work, we have quantified the toxicity of metallic nanoparticles in two cell lines by determining the IC_{50} values in MTT assay (3-(4,5-dimethylthiazol-2- yl)-2,5-diphenyltetrazolium bromide).

The activity of metallic nanoparticles against cells shows in Figure 7 A and B which is considered. After we added different concentration of metallic nanoparticle inhibits the Hep G 2 and AGS cell proferations that are indicated in the Graphical representation. At concentrations higher than 20µg /ml, they became necrotic and detached from the culture dishes. The dramatic changes induced by metallic nanoparticles at concentrations of 20 µg/ml and above were studied.

***In vitro* cytotoxicity of cancer cell line A) Hep G2 cell line B) AGS cell line.**

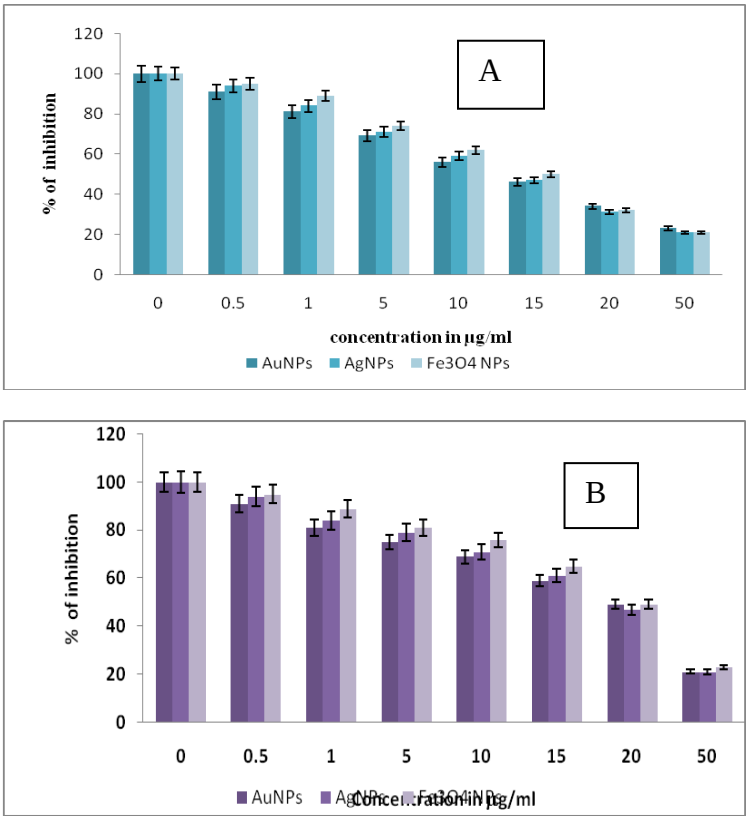

Figure 3.7 shows *In vitro cytotoxicity A) Hep G2 cell line and B) AGS cell line* analysis of the metal (Au,Ag & Fe_3O_4 NPs) nanoparticles.

CONCLUSION

We have successfully synthesised using the wet chemical synthesis route from their precursor salts has been used to synthesize nanoparticles using auric chloride, silver nitrate, Ferric sulphate and ferrous sulphate as an inorganic salts, trisodium citrate as a reducing agent for synthesis of gold and silver nanoparticles , further magnetic nanoparticles were obtained using the co precipitation techniques. The fabricated metallic nanoparticles were characterized by UV spectroscopy , Fourier-transform-infrared Spectroscopy (FTIR) analysis was used confirm the formation of the nanoparticles anmd they morphological analysis using x-ray diffraction (XRD), Scanning Electron Microscope (SEM) equipped with EDAX for determination of size, shape and their composition. After the characterization of the metallic nanoparticles they were analyzed for the antibacterial activity against four pathogens and cytotoxicity against Hep G2 and AGS cell line, where the IC_{50} value was calculated and the silver nanoparticles proved to be highly potiential followed by the gold nanoparticles and then the iron oxide nanoparticles. Thus all the three chemically synthesized nanoparticles proved to have potential biological applications.

Further the synthesized metallic nanoparticles were made as nanocomposite and used as platform for the biosensing applications. r

Conflict of interest

The authors declare no conflict of interest.

ACKNOWLEDGEMENT

One of the author N.Krithiga thank the DST inspire for the fellowship, UPE scheme for SEM image, DST purse, USIC, for the necessary instrumental facility in Madurai Kamaraj university, Madurai-21

REFERENCES

1. Naik AB, and Selukar NB, (2007). Does the antimicrobial activity of silver nanoparticles depend on the shape of the nanoparticles? A study of the Gram-negative bacterium Escherichia coli. *Applied Environ. Microbiol*, 73: 1712-1720.
2. Malhotra R, (2010). Mass spectroscopy in life sciences. *Curr. Sci*, 98: 140-145.
3. Balaji S (2010). Nanobiotechnology. MJP Publishers Chennai.
4. Mohanpuria P, *et al.*, (2007). *Journal of nanoparticle research*, 7:9275-9280.
5. Sastry M, *et al.*, (2003). *Current science*, 85:162-170.
6. Cheng TW, *et al.*, (2008). *Rev.Adv.Mater.Sci.*,18: 750-756.
7. Ho Chan *et al.*, (2008). *Rev.Adv.Mater.Sci. Sci*,. 18: 734.
8. Khandelwal N, Singh A, Jain D, Upadhyay MK and Verma HN, (2010). Green synthesis of silver Nanoparticles using *Argimone mexicana* leaf extract and Evaluation of their Antimicrobial activities. *Digest.J.Nanomater. Biostruct*, 5: 483-489
9. Sobha DK, *et al.*, (2010). *J.Biotech. Mol.Bio.Rev.* 5(1): 001-012.
10. Rai M, *et al.*, (2009). *Biotechnol., Adv.*, 27: (76-83).
11. Fang J, Zhang C and Mu R, (2005).The study of deposited silver particulate films by simple method for efficient SERS. *Chemical Physics Letters*, 401: 271-275.
12. Pan C, Hu B,Li W,Sun Y, Ye H and zeng X (2009), novel and efficient method for immobilization and stabilization of ß galactosidase by covalent .attachment onto magnetic nanoparticles Fe3O4 –chitosan nanoparticle J.Mol. catal.B.enzyme, 61, 208-215.
13. Shankar S, Ahmad A. and Sastry M, (2003). Geranium leaf assisted biosynthesis of silver nanoparticles. *Biotechnology Prog.*, 19: 1627–1631.
14. Prema P, (2010). Chemical mediated synthesis of silver nanoparticles and its potential antibacterial application.
15. Savithramma N, Lingo Rao M and Suvarnalatha D, (2011). Evaluation of Antibacterial efficacy of Biologically synthesized silver nanoparticles using stem bark of *Boswellia ovalifoliolata Bal.* and *Shorea tumbuggaia Roxb*. *Journal of Biological Science*, 11(1): 39-45.
16. Dipankar C, Murugan S (2012) The green synthesis, characterization and evaluation of the biological activities of silver nanoparticles synthesized from Iresine herbstii leaf aqueous extracts. Colloids Surf B 98:112–119
17. Winterbourne, C.C., Hawkins, R.E., Brain, M and Carrel, R.W (1975). The estimation of red cell superoxide dismutase activity. J. Lab.chem.Med. 85, 337-341.
18. Elizabeth K, Rao MNA, 1990, Oxygen radical scavenging activity of curcumin. Int J Pharmaceut, 58; 237-240.
19. Green LC, Wagner DA, Glogowski J, Skipper PL. Wishnok JS, Tannenbaum SR. Analysis of nitrite and 15N in biological fluids. Anal Biochem 1982;126:31.
20. Hammond SM and Lambert, (1978). Antimicrobial actions, *Edward Arnld Ltd*, London, 8-9.
21. Pal S, Tak YK and Song JM, (2007). Does the antimicrobial activity of silver nanoparticlesdepend on the shape of the nanoparticle? A study of the Gram negative bacterium *Escherichia coli. Appl. Environ. Microbiol*, 73 (6): 1712-1720.
22. Satyajit D Sarker, *et al.*, (2007). *Methods*. 42(4):321–324.
23. Kirby WWM, Bauer AW, Sherris JC and Turck M, (1966). Antibiotic susceptibility testing by a standardized single disc method, *American Journal of Clinical Pathology*; 45: 493- 496.
24. Frens G, *et al.*, (1973). *Nature. Phys. Sci.*, 241, 20-22.
25. Link S, M.A. El-Sayed J. Phys. Chem. B, 103 (1999), p. 4212
26. Shankar S, Ahmad A. and Sastry M, (2003). Geranium leaf assisted biosynthesis of silver nanoparticles. *Biotechnology Prog.*, 19: 1627–1631.
27. Halliwell B, Gutteridge JMC. Cross CE. Free radicals, antioxidants and human disease: Where are we now? J Lab Clin Med 1992; 119: 598–620.
28. Sies H. Oxidative stress: oxidants and antioxidants. Exp Physiol. 1997; 82, 2: 291–295.
29. Park, J.S., Petreas, M., Cohn, B.A., Cirillo, P.M., Factor-Litvak, P., 2009. Hydroxylated PCB metabolites (OH-PCBs) in archived serum from 1950–60s California mothers: a pilot study. Environ. Int. 35, 937–942.
30. Zhou, Y., Kong, Y., Kundu, S., Cirillo, J.D., Liang, H., 2012. Antibacterial activities of gold and silver nanoparticles against Escherichia coli and bacillus Calmette-Gue´rin. J. Nanobiotechnol. 10, 19.
31. Amro, N.A., Kotra, L.P., Wadu-Mesthrige, K., Bulychev, A., Mobashery, S., Liu, G., 2000. High-resolution atomic force microscopy studies of the Escherichia coli outer membrane: structural basis for permeability. Langmuir 16, 2789–2796.

32. Applerot, G., Lellouche, J., Lipovsky, A., Nitzan, Y., Lubar, T.R., Gedanken, A., Banin, E., 2012. Understanding the antibacterial mechanism of CuO nanoparticles: revealing the route of induced oxidative stress. Small 8, 3326–3337.
33. Morones, J.R., Elechiguerra, J.L., Camacho, A., Ramirez, J.T., 2005. The bactericidal effect of silver nanoparticles. Nanotechnology 16, 2346–2353
34. Raffi, M., Hussain, F., Bhatti, T.M., Akhter, J.I., Hameed, A., Hasan, M.M., 2008. Antibacterial characterization of silver nanoparticles against E. coli ATCC-15224. J. Mater. Sci. Technol. 24, 192–196.
35. Rai, M., Yadav, A., Gade, A., 2009. Silver nanoparticles as a new generation of antimicrobials. Biotechnol. Adv. 27, 76–83.
36. 35 Wiegand, I.; Hilpert, K.; Hancock, R. E. W. Agar and Broth Dilution Methods To Determine the Minimal Inhibitory Concentration (MIC) of Antimicrobial Substances. Nat. Protoc. 2008, 3, 163–175.
37. Moyano, D. F.; Goldsmith, M.; Solfiell, D. J.; LandesmanMilo, D.; Miranda, O. R.; Peer, D.; Rotello, V. M. Nanoparticle Hydrophobicity Dictates Immune Response. J. Am. Chem. Soc. 2012, 134, 3965–3967.
38. Shrivastava S, Bera T, Roy A, et al. (2007). Characterization of enhanced antibacterial effects of novel silver nanoparticles. Nanotechnology 18:225103–12.
39. Kim YS, Song MY, Park JD, et al. (2010). Subchronic oral toxicity of silver nanoparticles. Part Fibre Toxicol 7:20–31.
40. Maribel G, Guzmán JD, Stephan G (2009). Synthesis of silver nanoparticles by chemical reduction method and their antibacterial activity. Int. J. Chem. Biol.Eng. 2 (3):104-111.
41. Ravikumar S, Gnanadesigan M, Suganthi P, Ramalakshmi A (2010) Antibacterial potential of chosen mangrove plants against isolated urinary tract infectious bacterial pathogens. Int J Med Med Sci 2(3):94–99.
42. Sondi, I., and Salopek-Sondi, B. (2004). Silver nanoparticles as antimicrobial agent: a case study on *E. coli* as a model for Gram-negative bacteria. *J. Colloid Interface Sci.* 275, 177–182. doi: 10.1016/j.jcis.2004.02.01.
43. Bindhu, M. R., & Umadevi, M. (2015). Antibacterial and catalytic activities of green synthesized silver nanoparticles. Spectrochimica Acta Part A: Molecular and Biomolecular Spectroscopy, 135, 373e378.
44. Ankanna, S. and Savithramma, N. (2011): Biological synthesis of silver nanoparticles by using stem of Shorea tumbuggaia Roxb. and its antimicrobial efficacy. Asian journal of pharmaceutical and clinical research., 4(2): 137-141.
45. Panacek A, Kvitek L, Prucek R, Kolar M, Vecerova R, Pizurova N, Sharma V K, Nevecna T and Zboril R 2006 Silver colloid nanoparticles: synthesis, characterization, and their antibacterial activity J. Phys. Chem. B 110 16248–53.
46. Qi, L.F., Xu, Z.R., Jiang, X., Hu, C.H., Zou, X.F., 2004. Preparation and antibacterial activity of chitosan nanoparticles. Carbohydrate Research 339, 2693–2700.
47. Lin YE, Vidic RD, Stout JE, McCartney CA, Yu VL. Inactivation of Mycobacterium avium by copper and silver ions. Water Res, 1998; 32(7): 1997-2000.

5487847845**1170229**